

Interband Optical Absorption in Crossed Electric and Magnetic Fields in Germanium

Q. H. F. VREHEN*

National Magnet Laboratory, † Massachusetts Institute of Technology, Cambridge, Massachusetts

(Received 28 October 1965)

The theory for interband optical absorption in semiconductors in crossed electric and magnetic fields is developed for the case of low electric field strengths by considering the electric potential as a perturbation on the magnetic level structure. For simple parabolic valence and conduction bands the results agree with those of Aronov, obtained from an exact solution of the effective-mass Schrödinger equation in crossed fields, but the present method has the advantage that it can be applied to complicated bands, such as the degenerate valence bands in germanium, whenever the energy levels and eigenfunctions in the absence of an electric field are known. Actual calculations are presented for the case of germanium. Experimentally, the optical absorption in crossed fields was studied using a modulation technique in which both the transmission in the absence of an electric field and the modulation of this transmission by an ac electric field are measured to obtain the electric-field-induced change in absorption coefficient $\Delta\alpha$. Strain-free as well as strained thin germanium samples were used in magnetic fields up to 96 kOe and electric fields up to 1000 V/cm. Both allowed transitions ($\Delta n=0, -2$ for germanium) and electric-field-induced forbidden transitions ($\Delta n=-3, -1, +1$) can be observed in these differential spectra. A good agreement between theory and experiment is obtained. It is shown that under favorable conditions the electron and hole masses can be determined separately from the differential spectra. It is also found that the electric-field-modulation technique can sometimes be used to study the allowed transitions with greater sensitivity than in the normal magneto-absorption experiments.

In zero magnetic field the Stark broadening of the low-energy direct exciton line in a strained germanium sample was studied up to 1000 V/cm. The linewidth was found to vary linearly with electric field, increasing at a rate of about 160×10^{-8} eV/V cm⁻¹. This phenomenon is tentatively explained in terms of an electric dipole moment of the short-lived exciton state.

I. INTRODUCTION

THE theory of optical absorption in semiconductors in crossed electric and magnetic fields for direct interband transitions between simple parabolic bands was first formulated by Aronov.¹ The main implications of his results are discussed in the next section. We decided to investigate cross-field magnetoabsorption experimentally and chose germanium as the material to be studied since the structure of its valence and conduction bands seems to be known with more accuracy than that of any other semiconductor. However, the valence band in germanium is degenerate and therefore Aronov's theory cannot be applied. For that reason we developed a perturbation treatment, valid for relatively small electric fields, that can be applied to simple bands as well as to complicated bands. This treatment is similar to the one given by Hensel and Peter² when dealing with the problem of the Stark effect for cyclotron resonance in degenerate bands. These authors, however, limited their calculation to the Stark shifts of the Landau levels, whereas we study both these shifts and the effects of the electric field on the transition probabilities for interband optical transitions. This theory is presented in two subsequent sections, the first devoted to the case of simple bands and the second to that of germanium. A section on experimental techniques is mainly concerned with the preparation of

samples. In order to observe the small changes in optical absorption introduced by the application of a small electric field we used a differential method, in which an ac field is applied and the resulting modulation in transmission measured. A modulation in transmission of 1% can be very easily studied in this way. The characteristics of the differential spectra for cross-field magnetoabsorption are discussed in a separate section, assuming Landau line shapes, i.e., neglecting exciton effects. Since exciton effects actually are known to be important in germanium, we did experiments on the effect of an electric field on the exciton absorption lines in germanium (for zero magnetic field). Stark broadening was observed and the influence of this effect on the differential spectra is discussed briefly. In a final section we present the experimental results both for strained and strain-free germanium samples. A good agreement with theory is obtained.

II. EXACT THEORY FOR SIMPLE PARABOLIC BANDS

The optical absorption in semiconductors due to direct transitions between simple parabolic valence and conduction bands having their extrema at $k=0$ in crossed electric and magnetic fields was first studied theoretically by Aronov.¹ The Schrödinger equation for electrons and holes in crossed fields can be solved exactly for nondegenerate parabolic bands, and from the eigenfunctions so obtained the optical absorption can be derived in the same way as it was done for the case of a magnetic field alone by Roth *et al.*³ and Burstein and

³ L. M. Roth, B. Lax, and S. Zwerdling, *Phys. Rev.* **114**, 90 (1959).

* Address after 1 February 1966: Philips Research Laboratories, Eindhoven, The Netherlands.

† Supported by the U. S. Air Force Office of Scientific Research.

¹ A. G. Aronov, *Fiz. Tverd. Tela* **5**, 552 (1963) [English transl.: *Soviet Phys.—Solid State* **5**, 402 (1963)].

² J. C. Hensel and M. Peter, *Phys. Rev.* **114**, 411 (1959).

co-workers.⁴ The main results of Aronov's theory are as follows: First, the selection rule $\Delta n=0$, valid for $E=0$, breaks down in an electric field and transitions corresponding to $\Delta n=\pm 1, \pm 2, \dots$ have a finite transition probability. Secondly, all transitions are shifted to lower photon energies by an amount

$$\left(\frac{m_1+m_2}{2}\right)c^2\frac{E^2}{H^2},$$

where m_1 and m_2 are the electron and hole effective masses, and c is the velocity of light. Aronov proposed the measurement of this shift, which should yield a value for the sum of the masses of hole and electron. Combined with the value of the reduced mass $m_1m_2/(m_1+m_2)$ that can be found from the period of the oscillations in the normal magnetoabsorption spectrum the values of m_1 and m_2 can then be determined separately. Indeed, it has been shown experimentally by the present author⁵ that in germanium the optical transition between the zeroth Landau levels in valence and conduction bands can be shifted to a photon energy below the gap by a sufficiently strong electric field. From the magnitude of the shift as a function of electric and magnetic field it was concluded that a light-hole-to-electron transition was involved in that particular case. Fairly high electric fields ($\sim 3 \times 10^4$ V/cm) were needed to obtain measurable shifts.

We would like to point out that the same information can, in principle at least, be obtained from a study of the optical absorption above the gap in relatively low electric fields. It follows from Aronov's work that for small E , forbidden⁶ transitions $\Delta n=\pm k$ have a strength proportional to E^{2k} , so that only $\Delta n=\pm 1$ need be considered. With the differential technique described by Vrehan⁵ and Lax⁷ and more fully discussed in the present paper such forbidden transitions can be readily observed. Since, for these low electric fields, the electric-field-induced shifts can be neglected, the values of m_1 and m_2 can then be obtained from the positions of the allowed transitions $\Delta n=0$ and the forbidden transitions $\Delta n=\pm 1$. Besides the fact that low electric fields can be more easily applied to semiconductors than high fields, there is a more fundamental reason to work with low electric fields. In high electric fields many more transitions become possible. Since the absorption lines are usually broad, even in zero electric field only part of the structure is resolved. With many more lines present

in an electric field, it becomes more difficult to resolve the lines, and the net effect of the electric field is then to smooth out the magnetic structure completely. This is evident from previous work,⁵ where the main absorption peak becomes less pronounced as E increases. Experimental data presented in a later section of this paper also prove this point. Aronov has given the following expression for the absorption coefficient⁸:

$$\alpha = \frac{KH}{\omega} \exp\left(-\frac{a^2}{2}\right) \sum_{n,n'} (2^{n+n'} n! n'!)^{-1} \times \left| \sum_{m=0} b_m(n,n') a^{n+n'-2m} \right|^2 g(\omega - \omega_{nn'}), \quad (1)$$

where K is a constant:

$$K = \frac{2e^3}{\hbar^{5/2} n c^2 m^2} \left(\frac{2m_1 m_2}{m_1 + m_2}\right)^{1/2} (\mathbf{p}_{12} \cdot \mathbf{e})^2.$$

H is the magnetic field, ω the photon frequency. $g(\omega - \omega_{nn'})$ is the line shape for a transition between individual Landau sub-bands, centered at $\omega_{nn'}$, n and n' being the quantum numbers for the particular valence and conduction band Landau levels, respectively. For infinite relaxation time $g(\omega - \omega_{nn'}) = (\omega - \omega_{nn'})^{-1/2}$. The summation over m extends to n or n' , whichever is smaller,

$$b_m(n,n') = \frac{(-1)^{n'-m} n! n'! 2^m}{m!(n-m)!(n'-m)!}$$

and

$$a = eEL_M/\hbar\omega_c,$$

e is the proton charge, E the electric field strength and L_M the radius of the Landau orbit: $L_M = (\hbar c/eH)^{1/2}$. We define m_1 and m_2 as the masses of electron and hole, respectively, ω_{c1} and ω_{c2} are the corresponding cyclotron resonance frequencies. $\omega_c = \omega_{c1}\omega_{c2}/(\omega_{c1} + \omega_{c2})$ and $\Omega_c = \omega_{c1} + \omega_{c2}$.

$$\omega_{nn'} = \mathcal{E}g + (n' + \frac{1}{2})\hbar\omega_{c1} + (n + \frac{1}{2})\hbar\omega_{c2} - \frac{1}{2}(m_1 + m_2)c^2(E^2/H^2), \quad (2)$$

$\mathcal{E}g$ is the gap energy. Limiting ourselves to small E values, i.e., $a < 1$, we may expand Aronov's results in powers of a^2 , and retain only terms of order a^2 and lower, which gives

$$\alpha = \frac{KH}{\omega} \sum_{n,n'} P_{n,n'} g(\omega - \omega_{nn'}). \quad (1a)$$

$P_{n,n'}$ is, in the present approximation, different from

⁸ It should be pointed out that in Aronov's paper (Ref. 1) the right-hand side of Eq. (6) should be multiplied by a factor $(2^{n+n'} n! n'!)^{-1}$. In the same equation the summation over m should extend to the smallest of n and n' , not to $n'+1$. These mistakes have erroneously been taken over in Ref. 7. We have also divided Aronov's result by $2\pi^2$.

⁴ E. Burstein, G. S. Picus, R. F. Wallis, and F. Blatt, Phys. Rev. **113**, 15 (1959).

⁵ Q. H. F. Vrehan, Phys. Rev. Letters **14**, 558 (1965).

⁶ Throughout this paper the term "allowed transitions" will be used for transitions that are allowed in the absence of an electric field, whereas we shall call "forbidden transitions" those transitions that are forbidden for $E=0$, but obtain a finite probability for $E \neq 0$.

⁷ Q. H. F. Vrehan and B. Lax, Phys. Rev. Letters **12**, 471 (1964).

zero only for $\Delta n \equiv n' - n = 0, \pm 1$ and we have

$$\begin{aligned} P_{n,n-1} &= P_{n-1,n} = (n/2)a^2, \\ P_{n,n} &= 1 - [(2n+1)/2]a^2. \end{aligned} \quad (3)$$

It may be noted that $P_{n,n-1} + P_{n,n} + P_{n,n+1} = 1$, independent of electric field. Obviously, as long as the electric field is low enough, so as not to mix the two bands, the total transition probability from one band to the other should be independent of electric field.

III. PERTURBATION THEORY FOR SIMPLE BANDS

In the preceding section we obtained expressions for the optical absorption in crossed fields in the limit of low electric fields by expanding the exact expressions derived by Aronov. One can also arrive at these expressions by considering the electric potential as a perturbation on the level structure in a magnetic field and applying standard second-order perturbation theory. The criterion for the perturbation theory to be valid is $a \ll 1$. Such a treatment has the advantage that it can be extended to more complicated bands, such as the degenerate valence bands in germanium, or to non-parabolic bands, as long as the eigenfunctions and energy levels for the zero-electric-field case are known. In this section we shall discuss this theory for simple bands. In the effective-mass approximation the wave function of an electron in a magnetic field can be written as

$$\Psi_{in}(\mathbf{r}, k_{x_i}, k_{z_i}) = [1/(L_x L_z)^{1/2}] \exp(ik_{x_i}x + ik_{z_i}z) \Phi_n[(y/L_M) - L_M k_{x_i}] u_{i0}(\mathbf{r}), \quad (4)$$

where i refers to the particular band and n to the Landau level in question, L_x and L_z are the dimensions of the crystal along x and z , Φ_n is the normalized harmonic-oscillator wave function and u_{i0} the Bloch function at $\mathbf{k}=0$. The magnetic field is parallel to the z direction. With the electric field along y the potential energy for an electron is $V = eEy$ (e is the proton charge) and we have to calculate matrix elements like

$$\frac{1}{L_x L_z} \int \exp(-ik_{x_i}'x_i - ik_{z_i}'z_i) \Phi_{n'}^* u_{i0}'^* eEy \times \exp(ik_{x_i}x_i + ik_{z_i}z_i) \Phi_n u_{i0} d\mathbf{r}. \quad (5)$$

The u_{i0} have the periodicity of the lattice. Since all other functions involved vary only slightly within one unit cell we may approximate this integral by [a more careful evaluation of the integral (5) is given in Appendix B]:

$$\frac{1}{V_0 L_x L_z} \int_{\text{unit cell}} u_{i0}'^* u_{i0} d\mathbf{r} \times \int_{\text{crystal}} \exp(-ik_{x_i}'x_i - ik_{z_i}'z_i) \Phi_{n'}^* eEy \times \exp(ik_{x_i}x_i + ik_{z_i}z_i) \Phi_n d\mathbf{r}, \quad (6)$$

where V_0 the volume of the unit cell. In order for this matrix element to be different from zero we must have $k_{x_i} = k_{x_i}'$ and $k_{z_i} = k_{z_i}'$ and we obtain finally

$$\begin{aligned} & \int \Psi_{in'}^*(\mathbf{r}, k_{x_i}, k_{z_i}) eEy \Psi_{in}(\mathbf{r}, k_{x_i}, k_{z_i}) d\mathbf{r} \\ &= \int \Phi_{n'}^* \left(\frac{y}{L_M} - k_{x_i} L_M \right) eEy \Phi_n \left(\frac{y}{L_M} - k_{x_i} L_M \right) dy \\ & \equiv \langle n' | eEy | n \rangle. \end{aligned} \quad (7)$$

We did not consider matrix elements between Landau levels in different bands. In the present case these matrix elements would correspond to the mixing of two non-degenerate bands, i.e., the Zener effect, but this effect can be neglected for low electric fields. Computation of the integrals gives

$$\begin{aligned} \langle n | eEy | n-1 \rangle &= \langle n-1 | eEy | n \rangle = eEL_M (n/2)^{1/2}, \\ \langle n | eEy | n \rangle &= eEL_M^2 k_{x_i}, \\ \langle n | eEy | n' \rangle &= 0 \quad \text{for } |n-n'| > 1. \end{aligned} \quad (8)$$

From these matrix elements we readily obtain first-order perturbed wave functions and second-order energy perturbations.

For the conduction band we have

$$|(n_c)'\rangle = N_n^c \{ |n_c\rangle + V_{n,n-1}^c |(n-1)_c\rangle + V_{n,n+1}^c |(n+1)_c\rangle \}, \quad (9)$$

where a prime over a group of quantum numbers indicates a perturbed wave function, c stands for the conduction band, and N_n^c is a normalization factor:

$$\begin{aligned} N_n^c &\approx 1 - \frac{1}{2} \{ (V_{n,n-1}^c)^2 + (V_{n,n+1}^c)^2 \}, \\ V_{n,n-1}^c &= \frac{eEL_M (n/2)^{1/2}}{\hbar\omega_{c1}}, \quad V_{n,n+1}^c = \frac{eEL_M [(n+1)/2]^{1/2}}{-\hbar\omega_{c1}}. \end{aligned} \quad (10)$$

Similar expressions hold for the valence band. The energy perturbation of the levels in the conduction band to second order is

$$\Delta \mathcal{E}_n^c = eEL_M^2 k_{x_i} - (m_1/2)c^2(E^2/H^2), \quad (11)$$

and for the valence band,

$$\Delta \mathcal{E}_n^v = eEL_M^2 k_{x_i} + (m_2/2)c^2(E^2/H^2). \quad (12)$$

Energy shifts as predicted by this perturbation theory are therefore the same as those from the exact theory. It follows from the theory for magnetoabsorption that for direct transitions between simple bands the relative strengths of the various transitions are proportional to the square of the product of the envelope functions of the initial and final states. For $E=0$ this leads to the selection rules: $\Delta k_z = \Delta k_x = 0$ and $\Delta n = 0$. Evaluating these products for the first-order perturbed envelope functions we find the selection rules $\Delta k_z = \Delta k_x = 0$ and $\Delta n = 0, \pm 1$. The relative strengths of these transitions

are

$$P_{n,n-1} = P_{n-1,n} = |\langle (n_v)' | \{ (n-1)_c \}' \rangle|^2 = (n/2)a^2, \quad (13)$$

$$P_{n,n} = |\langle (n_v)' | (n_c)' \rangle|^2 = 1 - [(2n+1)/2]a^2$$

and this is again the same result as from the exact theory.

IV. PERTURBATION THEORY FOR GERMANIUM

In germanium the valence band is degenerate at $k=0$. Aronov's theory cannot be applied to this case. On the other hand, the perturbation treatment discussed in the previous section can be extended for this more complex problem, provided the wave functions and energy levels for $E=0$ are known. The problem of energy levels and wave functions of a degenerate band in a magnetic field was studied by Luttinger and Kohn.⁹ Their results were extended by various authors, including Roth,³ Goodman,¹⁰ and Evtuhov.¹¹ We shall closely follow Roth's work. Wave functions and energies at $k_z=0$ are of most interest to us, since they determine the strength and positions of peaks in the magnetoabsorption spectrum.¹² At $k_z=0$ the valence-band wave functions can be written in Roth's notation as

$$\begin{aligned} |na\pm\rangle &= a_{1,n}^\pm \varphi_{n-2}(\mathbf{r})u_{10} + a_{2,n}^\pm \varphi_n(\mathbf{r})u_{20}, \\ |nb\pm\rangle &= b_{1,n}^\pm \varphi_{n-2}(\mathbf{r})u_{30} + b_{2,n}^\pm \varphi_n(\mathbf{r})u_{40} \end{aligned} \quad (14)$$

$$\begin{aligned} \langle n a i | e E y | n' a j \rangle &= A_{n,n'}^{ij} e E L_M, \\ A_{n,n-1}^{ij} &= a_{1,n}^i a_{1,n-1}^j [(n-2)/2]^{1/2} + a_{2,n}^i a_{2,n-1}^j (n/2)^{1/2}, \\ A_{n,n+1}^{ij} &= a_{1,n}^i a_{1,n+1}^j [(n-1)/2]^{1/2} + a_{2,n}^i a_{2,n+1}^j [(n+1)/2]^{1/2}; \end{aligned} \quad (19)$$

i and j run both over $+$ and $-$. $A_{n,n'}^{ij} = 0$ for $|n-n'| > 1$. For the b series we replace the a 's by b 's and A 's by B 's. The unperturbed energies of the various levels we indicate by $\mathcal{E}_n^{a\pm}$ and $\mathcal{E}_n^{b\pm}$ and we define

$$\epsilon_{n,n'}^{aij} = (\hbar e H / mc)^{-1} \{ \mathcal{E}_n^{ai} - \mathcal{E}_{n'}^{aj} \}.$$

With this definition the second-order shift for the n th light-hole level in the a series is given by

$$\Delta_2 \mathcal{E}_n^{a+} = \frac{mc^2 E^2}{H^2} \left\{ \frac{A_{n,n-1}^{++} + A_{n,n+1}^{++}}{\epsilon_{n,n-1}^{a++} + \epsilon_{n,n+1}^{a++}} + \frac{A_{n,n-1}^{+-} + A_{n,n+1}^{+-}}{\epsilon_{n,n-1}^{a+-} + \epsilon_{n,n+1}^{a+-}} \right\}. \quad (20)$$

⁹ J. M. Luttinger and W. Kohn, Phys. Rev. **97**, 869 (1955); J. M. Luttinger *ibid.* **102**, 1030 (1956).

¹⁰ R. R. Goodman, Phys. Rev. **122**, 397 (1961).

¹¹ V. Evtuhov, Phys. Rev. **125**, 1869 (1962).

¹² Evtuhov (Ref. 11) has shown that crossing can take place at $k_z \neq 0$. Near the crossover points the present perturbation theory is not valid. However, crossing takes place at relatively large values of k_z , which are of little concern to us. We neglect these difficulties.

and the conduction-band functions

$$|n\alpha\rangle = \varphi_n(\mathbf{r})S_\alpha \quad \text{and} \quad |n\beta\rangle = \varphi_n(\mathbf{r})S_\beta. \quad (15)$$

The coefficients $a_{i,n}^\pm$ and $b_{i,n}^\pm$, where $+$ and $-$ stand for light and heavy holes, respectively, can be obtained from the secular equations for the energy. The u_{j0} are Bloch functions for the valence band, S for the conduction band, α and β indicate spin up and down,

$$\varphi_n(\mathbf{r}) = \frac{1}{(L_x L_z)^{1/2}} \exp(ik_x x) \Phi_n \left(\frac{y}{L_M} - L_M k_x \right). \quad (16)$$

Let us now consider the matrix elements of the electric potential between the valence band states. Since these matrix elements contain the products of the Bloch functions, as argued before, we see immediately that those between a and b series states vanish. In other words, the electric field does not mix the a and b series.¹³⁻¹⁵ Furthermore, it follows from the orthonormality of the various states

$$\langle na\pm | e E y | na\mp \rangle = \langle nb\pm | e E y | nb\mp \rangle = 0, \quad (17)$$

$$\langle na\pm | e E y | na\pm \rangle = \langle nb\pm | e E y | nb\pm \rangle = e E L_M^2 k_x. \quad (18)$$

The last line shows that in first order all the levels undergo the same shift, and this shift is equal to that for simple bands:

We furthermore define

$$V_{n,n'}^{aij} = \frac{A_{n,n'}^{ij}}{\epsilon_{n,n'}^{aij}}, \quad \text{and} \quad C = \frac{L_M m c}{\hbar H},$$

where m is the free-electron mass.

The first-order perturbed wave function for the n th light-hole level can now be written as

$$|(na+)' \rangle = N_n^{a+} \{ |na+\rangle + (\sum_{n',j} V_{n,n'}^{a+j} |n'a j \rangle) C E \}, \quad (21)$$

n' takes on the values $n-1$ and $n+1$; j runs over $+$ and $-$. N_n^{a+} is again a normalization factor, which, in

¹³ When the warping of the energy surfaces is taken into account fully, the eigenfunctions are linear combinations containing all four band edge Bloch functions $u_{10} \cdots u_{40}$. The electric field then does mix the a and b series. This effect, however, is small for germanium. Recently, Shindo (Refs. 14 and 15) has calculated the Stark shifts of the valence-band Landau levels in germanium, taking into account the warping of the energy surfaces correctly. The author is grateful to Dr. Shindo for sending him a preprint of his work.

¹⁴ T. Shindo, in *Proceedings of the 7th International Conference on the Physics of Semiconductors, Paris 1964* (Dunod Cie., Paris, 1964).

¹⁵ T. Shindo, J. Phys. Chem. Solids **26**, 1431 (1965).

the present approximation has the value

$$N_n^{a+} = 1 - \frac{1}{2}C^2E^2 \sum_{n',j} (V_{n,n'}^{a+j})^2 \equiv 1 - \frac{1}{2}K_n^{a+}C^2E^2. \quad (22)$$

Similar expressions hold for the heavy-hole states of the a series and for light and heavy holes in the b series. For the conduction band we write the perturbed wave functions as

$$|(n\alpha)' \rangle = N_n^{\alpha} \{ |n\alpha \rangle + (V_{n,n-1}^{\alpha} |n-1, \alpha \rangle + V_{n,n+1}^{\alpha} |n+1, \alpha \rangle) CE \} \quad (23)$$

and similarly for β . In the conduction band, of course, the electric field does not couple α states with β states. The coefficients N_n^{α} , $V_{n,n-1}^{\alpha}$, and $V_{n,n+1}^{\alpha}$ can be obtained from the theory for simple bands.

The matrix elements for optical transitions between the perturbed states in valence and conduction band can now be expressed in terms of those for the unperturbed states. The latter are known from Roth's work. We define the following operators, corresponding to polarized radiation in the σ_+ , σ_- , and π configuration¹⁶

$$\begin{aligned} \sigma_+ &\equiv \frac{p_x - ip_y}{\langle X | p_x | S \rangle \sqrt{2}}, \\ \sigma_- &\equiv \frac{p_x + ip_y}{\langle X | p_x | S \rangle \sqrt{2}}, \\ \pi &\equiv \frac{p_z}{\langle X | p_x | S \rangle}. \end{aligned}$$

Then the matrix elements governing the direct interband transitions are given by

$$\begin{aligned} \langle na \pm | \sigma_- | n-2, \alpha \rangle &= +a_{1,n}^{\pm}, \\ \langle na \pm | \sigma_+ | n\alpha \rangle &= -(1/\sqrt{3})a_{2,n}^{\pm}, \\ \langle nb \pm | \sigma_+ | n\beta \rangle &= +b_{2,n}^{\pm}, \\ \langle nb \pm | \sigma_- | n-2, \beta \rangle &= -(1/\sqrt{3})b_{1,n}^{\pm}, \\ \langle na \pm | \pi | n\beta \rangle &= -(2/\sqrt{6})a_{2,n}^{\pm}, \\ \langle nb \pm | \pi | n-2, \alpha \rangle &= +(2/\sqrt{6})b_{1,n}^{\pm}. \end{aligned} \quad (24)$$

Generally speaking, for $E=0$, two types of transitions are allowed, namely $\Delta n=0$ and $\Delta n=-2$. In an electric field the intensity of these transitions is decreased whereas formerly forbidden transitions $\Delta n=-3, -1, +1$ now obtain a finite transition probability. For $E=0$, for a given series (a or b) and for a given polarization (σ_+, σ_- or π) only one type of transition occurs: either $\Delta n=-2$ or $\Delta n=0$. In an electric field this transition is decreased in intensity and forbidden transitions $\Delta n=-3, -1$, or $\Delta n=-1, +1$ are introduced, respectively.

Experimentally, we applied a differential technique. For the allowed transitions we are interested in the

¹⁶ We use the conventional notation: σ_+ corresponds to left-handed circular polarization, absorption of a σ_+ photon to a transition $\Delta m = +1$. Roth apparently adopted the opposite notation.

change in the square of the matrix element due to the electric field, whereas for the forbidden ones we are interested in the electric-field-induced intensity itself, all to second power in E . Formulas were derived by the present author for transitions from both the a and b series and for the three polarizations σ_+, σ_- , and π . The results for σ_- and light holes in the a series are

$$|\langle (na+)' | \sigma_- | (n-2 \pm 1, \alpha)' \rangle|^2 = E^2 C^2 \{ a_{1,n \pm 1}^+ V_{n,n \pm 1}^{a++} + a_{1,n \pm 1}^- V_{n,n \pm 1}^{a+-} + a_{1n}^+ V_{n-2 \pm 1, n-2}^{\alpha} \}^2, \quad (25a)$$

$$-\Delta |\langle (na+)' | \sigma_- | (n-2, \alpha)' \rangle|^2 \approx |\langle (na+)' | \sigma_- | (n-3, \alpha)' \rangle|^2 + |\langle (na+)' | \sigma_- | (n-1, \alpha)' \rangle|^2, \quad (25b)$$

where

$$\begin{aligned} \Delta |\langle (na+)' | \sigma_- | (n-2, \alpha)' \rangle|^2 &= |\langle (na+)' | \sigma_- | (n-2, \alpha)' \rangle|^2 - |\langle na+ | \sigma_- | n-2, \alpha \rangle|^2. \end{aligned}$$

These expressions are correct to second power in E . On the right-hand side of Eq. (25b) we have omitted a number of terms which can all be proved to be small. These terms are fully discussed in Appendix A. The expressions for heavy holes are obtained by replacing everywhere $+$ by $-$ and vice versa; those for the b series by replacing a by b , α by β and multiplying the result by a factor $\frac{1}{3}$. For σ_+ radiation and transitions from light hole a series levels:

$$|\langle (na+)' | \sigma_+ | (n \pm 1, \alpha)' \rangle|^2 = \frac{1}{3} E^2 C^2 \{ a_{2,n \pm 1}^+ V_{n,n \pm 1}^{a++} + a_{2,n \pm 1}^- V_{n,n \pm 1}^{a+-} + a_{2,n}^+ V_{n \pm 1, n}^{\alpha} \}^2, \quad (26a)$$

$$-\Delta |\langle (na+)' | \sigma_+ | (n, \alpha)' \rangle|^2 \approx |\langle (na+)' | \sigma_+ | (n-1, \alpha)' \rangle|^2 + |\langle (na+)' | \sigma_+ | (n+1, \alpha)' \rangle|^2. \quad (26b)$$

The expressions for the b series follow from these by replacing a by b , α by β and multiplying the result by a factor of 3. Finally, for π transitions, we obtain

$$|\langle (na+)' | \pi | (n \pm 1, \beta)' \rangle|^2 = \frac{2}{3} E^2 C^2 \{ a_{2,n \pm 1}^+ V_{n,n \pm 1}^{a++} + a_{2,n \pm 1}^- V_{n,n \pm 1}^{a+-} + a_{2,n}^+ V_{n \pm 1, n}^{\beta} \}^2, \quad (27a)$$

$$-\Delta |\langle (na+)' | \pi | (n, \beta)' \rangle|^2 \approx |\langle (na+)' | \pi | (n-1, \beta)' \rangle|^2 + |\langle (na+)' | \pi | (n+1, \beta)' \rangle|^2, \quad (27b)$$

whereas now the transitions from the b series are given by

$$|\langle (nb+)' | \pi | (n-2 \pm 1, \alpha)' \rangle|^2 = \frac{2}{3} E^2 C^2 \{ b_{1,n \pm 1}^+ V_{n,n \pm 1}^{b++} + b_{1,n \pm 1}^- V_{n,n \pm 1}^{b+-} + V_{n-2 \pm 1, n-2}^{\alpha} b_{1,n}^+ \}^2, \quad (28a)$$

$$-\Delta |\langle (nb+)' | \pi | (n-2, \alpha)' \rangle|^2 \approx |\langle (nb+)' | \pi | (n-3, \alpha)' \rangle|^2 + |\langle (nb+)' | \pi | (n-1, \alpha)' \rangle|^2. \quad (28b)$$

For simple bands we found that the electric-field-induced decrease in intensity of the allowed transitions $n \rightarrow n$ just equals the sum of the intensities for the forbidden transitions $n \rightarrow n-1$ and $n \rightarrow n+1$. From Eqs. (25) through (28) we see that this is approximately true for germanium. A complete discussion of the transfer of transition probability is given in Appendix A.

The coefficients expressing the coupling between light and heavy holes, such as $V_{n,n-1}^{a+-} = (A_{n,n-1}^{+/-} / \epsilon_{n,n-1}^{a+-})$ are generally small for two reasons. First, since $a_{1,n-1}^{+}a_{1,n-1}^{-} + a_{2,n-1}^{+}a_{2,n-1}^{-} = 0$ and since the a 's vary smoothly with n , the numerators $A_{n,n-1}^{+/-} = a_{1,n-1}^{+}a_{1,n-1}^{-} [(n-2)/2]^{1/2} + a_{2,n-1}^{+}a_{2,n-1}^{-} (n/2)^{1/2}$ turn out to be relatively small. Secondly, the energy denominators $\epsilon_{n,n-1}^{a+-}$ are rather large (as compared to $\epsilon_{n,n-1}^{a++}$ or $\epsilon_{n,n-1}^{a--}$), especially for higher quantum numbers n . The coupling between light and heavy holes is thus seen to be rather weak. We have already established the fact that there is no coupling at all between the a and b series. This then means, that to a good approximation the electric field affects each of the four valence-band ladders separately and each ladder behaves under the influence of the electric field almost as a simple band, apart from quantum effects for small numbers n . Since now for simple bands the electric-field-induced transition probabilities are proportional to $(m_1+m_2)^2$ and since (m_1+m_2) is about 4 times larger for electron and heavy hole than for electron and light hole, one might expect the heavy-hole transitions to show up much more strongly in our differential spectra than the light-hole ones. We have indeed observed that the lines due to heavy-hole transitions are stronger in the differential spectra than in the magnetoabsorption spectra when compared with light-hole transitions. This predominance of the heavy-hole transitions, however, is not as pronounced as one would predict from the transition probabilities alone, a phenomenon that finds its explanation in the fact that for heavy holes the energies of forbidden transitions $\Delta n = \pm 1$ are very close to the energy for the allowed transition $\Delta n = 0$. This point is discussed further in the section on the characteristics of differential spectra.

V. EXPERIMENTAL TECHNIQUES

Most of the experiments were made on a sample of intrinsic germanium, mechanically polished to a thickness of 7μ , and freely mounted, i.e., not glued to a glass substrate. This was essential in order to prevent strains in the sample at low temperature¹⁷ which would invalidate the comparison of theory with experiment. To avoid heating of the sample on the application of an electric field, it was brought into direct contact with the liquid-nitrogen bath and only samples which showed a high resistivity at 77°K were used. The sample had a width of 2 mm, and a length of 2 mm between electrodes. Electrodes were attached to both ends of the sample. These electrodes must fulfill the following requirements:

- They must provide good electrical contacts, even at 77°K .
- They must allow the sample to contract freely when cooled down to 77°K .

¹⁷ G. G. Macfarlane, T. P. McLean, J. E. Quarrington, and V. Roberts, Phys. Rev. Letters 2, 252 (1959).

(c) Both the electrode and the conducting glue used to attach the electrode to the sample must be extremely thin, because otherwise the strains in the sample, set up in the contact region at cooling, will cause the sample to break.

The following solution proved to be very useful. The electrodes were applied to the sample before it was removed from the optical flat on which it had been mounted during the polishing process. First, a drop of Viking LS 232 liquid-metal alloy¹⁸ was put on both ends of the sample and left there for about 24 h. This material wets almost any surface and it alloys with the germanium so as to give a good metal to semiconductor contact. After 24 h most of the Viking LS 232 was removed and only a thin layer left. This was necessary both to obtain a thin structure (requirement *c*) and to prevent the ends of the germanium sample from eventually dissolving completely in the alloy. Next, strips of $2\text{-}\mu$ -thick gold foil were glued to the contact areas with the conductive cement Eccobond 57C.¹⁹ This material sets at room temperature in about 8 h, and, when properly diluted, can be used in layers as thin as 1μ . The sample was then removed with acetone from the

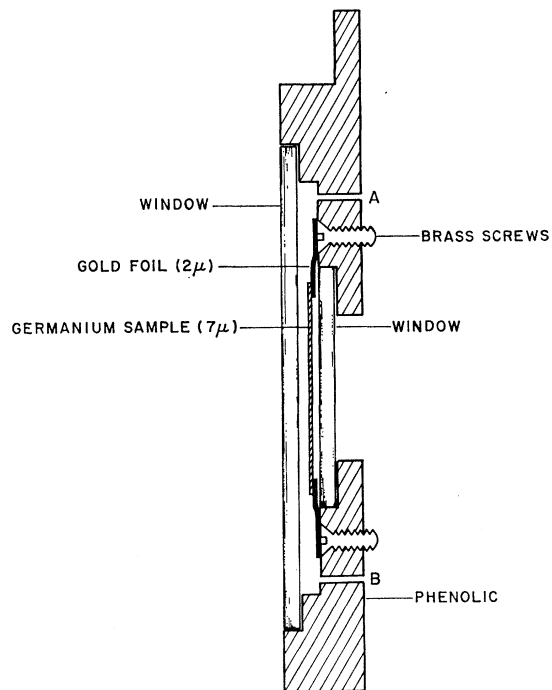


FIG. 1. Sketch of sample holder. The $7\text{-}\mu$ -thick germanium sample is placed between two fused-silica windows. Thin gold foils (2μ) connect the ends of the sample to brass screws from which copper wires run out of the Dewar for application of electric fields. The gold foils allow the sample to contract freely when cooled down. Small holes A and B let the cooling liquid enter the sample holder, but the sample is protected against violent bubbling of the cooling liquid.

¹⁸ A ternary eutectic of the mercury-indium-thallium system, marketed by Elmat Corporation, Mountain View, California.

¹⁹ Emerson and Cuming Inc., Canton, Massachusetts.

substrate and could be handled easily with tweezers at one of the gold foils attached to it. The sample was then put in a holder, with the gold foils glued to brass screws, to which copper wires were soldered for applying the electric fields. A diagram of the sample holder with sample mounted in it is given in Fig. 1. The sample is between two glass plates. Small holes allow liquid nitrogen to enter between these glass plates, but the sample is protected against damage from the violently boiling liquid present around the sample holder when the Dewar is being filled. A second sample backed onto a substrate and therefore strained at 77°K was used in some experiments, because it showed somewhat narrower absorption lines. This sample had a length of 15 mm (between electrodes), a width of 2 mm and a thickness of $7\ \mu$. For this sample we measured current versus voltage characteristics at 77°K (see Fig. 2). The current is a superlinear function of V . The resistance over the whole range was greater than 100 M Ω . It should be mentioned that we have little information about the uniformity of the electric field over the samples. Our main interest was in the spectral dependence of the differential absorption for a given voltage. In the low electric-field region the spectral variation of the differential absorption does not depend on electric field strength, although its magnitude varies as E^2 . Therefore, when the electric field is not completely uniform, various parts of the sample will still contribute the same differential spectrum but with possibly different magnitudes.

A Bitter-type magnet with a $2\frac{1}{8}$ -in. bore and a $1\frac{1}{8}$ -in. radial access hole was used, giving magnetic fields up to 96 kG at 5 MW. The sample was in the Faraday configuration, i.e., infrared radiation passed through the sample parallel to the magnetic field. A standard optical apparatus was employed, having a tungsten lamp as a source, a Perking-Elmer double pass grating monochromator (equipped with a $1.6\text{-}\mu$ Bausch and Lomb grating) in the fore-optics and a lead sulfide detector. Signals were amplified with a Tektronix 122 pre-amplifier, rectified with the Princeton JB4 phase-sensitive amplifier and fed into a recorder.

Electric fields up to about 1000 V/cm could be applied. The differential spectra were obtained by first measuring the transmitted intensity I with no electric field present (this was done with the light beam interrupted periodically by a chopper) and next measuring the modulation in the transmitted intensity ΔI due to an oscillating electric field (the light beam not being chopped now). The differential absorption coefficient $\Delta\alpha$ is then given by $\Delta\alpha = -(1/d)(\Delta I/I)$, where d is the thickness of the sample (see next section).

VI. CHARACTERISTICS OF DIFFERENTIAL SPECTRA

Neglecting interference effects, which are small indeed if $\alpha d > 1$ (α the absorption coefficient, d sample

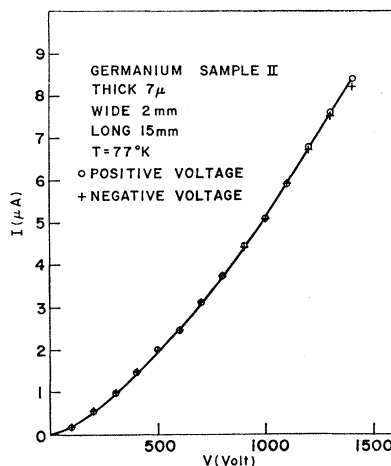


Fig. 2. Current-voltage characteristics for germanium sample II at 77°K. This sample has a thickness of $7\ \mu$, width of 2 mm and length of 15 mm between electrodes. The sample is backed to a glass substrate.

thickness), the transmitted intensity I is related to the incident intensity I_0 by

$$I = (1 - R)^2 I_0 \exp(-\alpha d), \quad (29)$$

where R is the reflection coefficient at the surface. If a small change $\Delta\alpha$ is introduced in the absorption coefficient, e.g., by an electric field, and if we neglect changes in R we find

$$\Delta\alpha = -(1/d)(\Delta I/I). \quad (30)$$

A plot of $(-\Delta I/I)$ as a function of photon frequency we shall call a differential spectrum. Expanding α as a function of E about $E=0$ one has

$$\alpha(E) = \alpha(0) + \frac{\partial\alpha}{\partial E}E + \frac{1}{2} \frac{\partial^2\alpha}{\partial E^2}E^2 + \dots \quad (31)$$

In the case of cross-field magnetoabsorption the linear term vanishes and we obtain

$$\Delta\alpha = \alpha(E) - \alpha(0) = \frac{1}{2} \frac{\partial^2\alpha}{\partial E^2}E^2 + \dots \quad (32)$$

Suppose we apply a dc electric field E_0 superimposed on which is an ac field $E_1 \cos\omega_0 t$. Then the differential absorption coefficient is

$$\Delta\alpha = \frac{1}{2} \frac{\partial^2\alpha}{\partial E^2} \left\{ \left(E_0^2 + \frac{E_1^2}{2} \right) + 2E_1 E_0 \cos\omega_0 t + \frac{E_1^2}{2} \cos 2\omega_0 t \right\} + \dots \quad (33)$$

which contains components both at the fundamental frequency and the second harmonic frequency. For the first of these, we find the amplitude

$$\Delta\alpha_{\omega_0} = E_1 E_0 (\partial^2\alpha/\partial E^2) + \dots \quad (34)$$

From Eq. (1) we see that the absorption spectrum consists of a superposition of individual absorption lines whose intensity $Q_{nn'}(E)$ and position $\omega_{nn'}(E)$ (as a function of photon frequency) are dependent on E , but whose line shapes are constant and equal for all of the lines.

$$\alpha(\omega, E) = \sum_{n, n'} Q_{nn'}(E) g(\omega - \omega_{nn'}(E)), \quad (35)$$

where $Q_{nn'}(E) = (KH/\omega)P_{nn'}$ and $\omega_{nn'}(E)$ is given by Eq. (2). Using the fact that $\partial Q_{nn'}/\partial E = \partial \omega_{nn'}/\partial E = 0$ at $E=0$, we find

$$\left(\frac{\partial^2 \alpha}{\partial E^2}\right)_{E=0} = \sum_{nn'} \left(\frac{\partial^2 Q_{nn'}(\omega)}{\partial E^2}\right)_{E=0} g(\omega - \omega_{nn'}(0)) + Q_{nn'}(0) \frac{\partial g(\omega - \omega_{nn'})}{\partial \omega_{nn'}} \left(\frac{\partial^2 \omega_{nn'}}{\partial E^2}\right)_{E=0}. \quad (36)$$

Transitions for which $Q_{nn'}(0) \neq 0$ are allowed in the absence of an electric field. For these transitions there are two contributions to the differential spectrum, one having the normal line shape $g(\omega - \omega_{nn'})$ and the other the derivative line shape $\partial g(\omega - \omega_{nn'})/\partial \omega_{nn'}$. Transitions for which $Q_{nn'}(0) = 0$ are forbidden in the absence of an electric field. These contribute lines of standard shape $g(\omega - \omega_{nn'})$ to the differential spectrum. In order to construct specific models for the differential spectra we now assume a line shape, following Roth³:

$$g(\omega - \omega_{nn'}) = \left\{ \frac{(\omega - \omega_{nn'}) + [(\omega - \omega_{nn'})^2 + (1/\tau^2)]^{1/2}}{2[(\omega - \omega_{nn'})^2 + (1/\tau^2)]} \right\}^{1/2},$$

$$\frac{\partial g(\omega - \omega_{nn'})}{\partial \omega_{nn'}} = \frac{2(\omega - \omega_{nn'}) - [(\omega - \omega_{nn'})^2 + (1/\tau^2)]^{1/2}}{2[(\omega - \omega_{nn'})^2 + (1/\tau^2)]} g(\omega - \omega_{nn'}). \quad (37)$$

The height of $g(\omega - \omega_{nn'})$ is proportional to $\tau^{1/2}$, that of $\partial g(\omega - \omega_{nn'})/\partial \omega_{nn'}$ is proportional to $\tau^{3/2}$. In Fig. 3

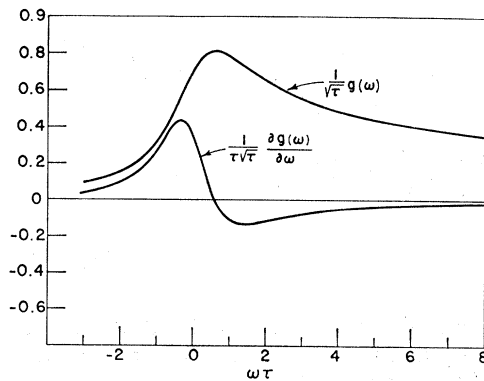


FIG. 3. Landau line shape $g(\omega)$ and its derivative, both normalized with respect to the relaxation time τ , as a function of $\omega\tau$.

we have plotted $(1/\tau^{1/2})g(\omega - \omega_{nn'})$ and $(1/\tau^{3/2}) \times [\partial g(\omega - \omega_{nn'})/\partial \omega]$ as functions of $(\omega - \omega_{nn'})\tau$. It is interesting to compare the relative magnitudes of the contributions to the differential spectrum proportional to $g(\omega - \omega_{nn'})$ and $\partial g(\omega - \omega_{nn'})/\partial \omega_{nn'}$ for a given allowed transition. Since $g(\omega - \omega_{nn'})$ and $(1/\tau)[\partial g(\omega - \omega_{nn'})/\partial \omega_{nn'}]$ have relative heights independent of τ , we have to compare $(\partial^2 Q_{nn'}/\partial E^2)_{E=0}$ with $\tau Q_{nn'}(0)(\partial^2 \omega_{nn'}/\partial E^2)_{E=0}$. For simple bands, one finds

$$\tau Q_{nn'}(0) \left(\frac{\partial^2 \omega_{nn'}}{\partial E^2}\right)_{E=0} / \left(\frac{\partial^2 Q_{nn'}}{\partial E^2}\right)_{E=0} = \frac{1}{2n+1} \omega_c \tau. \quad (38)$$

The contribution of the derivative line shape is, therefore, important only for $\omega_c \tau \gg 1$ and small values of n .

For simple bands we find from Eqs. (1a) and (3) the following expression:

$$\left(\frac{\partial^2 \alpha}{\partial E^2}\right)_{E=0} = \frac{K(m_1 + m_2)^2 c^3}{\omega \hbar e H^2} \times \tau^{1/2} G(\omega)$$

$$G(\omega) = \frac{1}{\tau^{1/2}} \sum_{n=0}^{\infty} \left[-(2n+1)g(\omega - \omega_{nn}) + ng(\omega - \omega_{n-1}) + (n+1)g(\omega - \omega_{n+1}) - \omega_c \tau \frac{1}{\tau} \frac{\partial g(\omega - \omega_{nn})}{\partial \omega_{nn}} \right]. \quad (39)$$

To study the influence of the parameters m_1 , m_2 , and $\omega_c \tau$ on the differential spectrum we calculated $G(\omega)$ for various values of these parameters.²⁰ We first took $m_2 = 2m_1$, which is the optimum situation for resolving both allowed and forbidden transitions, and $\Omega_c \tau = 27, 9, 3, 1$. The results are presented in Fig. 4. Three features are of importance. First, the contribution of the derivative line shape, resulting from the electric-field-induced shift of transition energy for allowed transitions, is appreciable for $\Omega_c \tau = 27$ but can be neglected for the lower values of $\Omega_c \tau$. Secondly, the forbidden transitions are only well resolved for $\Omega_c \tau > 9$. For smaller values of τ the differential spectrum shows broad oscillations with the same period as the normal magnetoabsorption spectrum, i.e., the period is determined by the reduced effective mass for electrons and holes. This indicates that the differential spectrum can be used to measure electron and hole mass separately only under rather favorable conditions, namely with a large value of $\Omega_c \tau$ and the ratio of the two masses close to 1:2. Thirdly, it is seen that the amplitude of the oscillations in $G(\omega)$ drops off sharply for $\Omega_c \tau$ near 1. This is even more pronounced for the differential spectrum itself, which is

²⁰ For the calculation of $G(\omega)$ a finite number of terms in the series was taken. Even though we were only interested in $G(\omega)$ in the neighborhood of the first few transitions, many more terms in the series had to be taken into account, especially for small $\Omega_c \tau$, in order to include properly the effect of tails of the higher transitions.

proportional to $\tau^{1/2}G(\omega)$. The physical reason for this is the following. The decrease in intensity for allowed transitions $\Delta n=0$ resulting from the application of an electric field just equals the increase in intensity of the forbidden transitions $\Delta n=\pm 1$, as we have seen before. If these transitions are broadened sufficiently to overlap, they will cancel out to a certain degree. In germanium this effect will be more pronounced for heavy-hole transitions than for light-hole transitions. In Sec. IV we found that heavy- and light-hole transitions can almost be treated separately. We therefore calculated the differential spectrum for simple bands, with the follow-

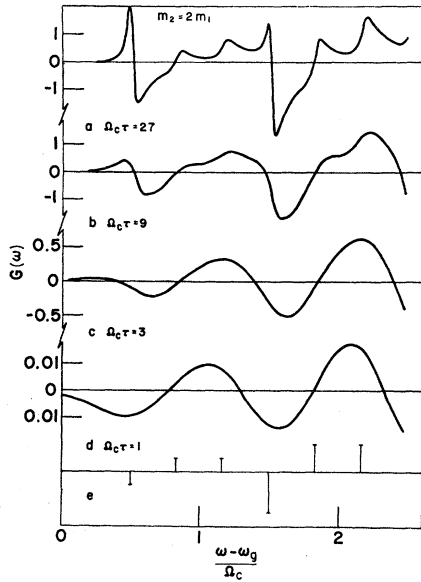


FIG. 4. The quantity $G(\omega)$ defined in Eq. (39) for $m_2=2m_1$ and for (a) $\Omega_c\tau=27$, (b) $\Omega_c\tau=9$, (c) $\Omega_c\tau=3$, (d) $\Omega_c\tau=1$. The position and relative intensity of the lines in the differential spectrum as calculated from perturbation theory is given in (e). Positive lines correspond to $\Delta n=\pm 1$ forbidden transitions, negative ones to $\Delta n=0$ allowed transitions. For $\Omega_c\tau=9$ and $\Omega_c\tau=27$ the forbidden transitions are resolved. The positive peaks just below the allowed transitions for $\Omega_c\tau=27$ are due to the presence of the derivative of the Landau line shape, which stems from the electric-field-induced shift in transition energy. Note the decrease in amplitude of the oscillations with decreasing $\Omega_c\tau$.

ing sets of parameters:

$$m_2 = m_1, \quad \omega_{c1}\tau = 4,$$

$$m_2 = 10m_1, \quad \omega_{c1}\tau = 4.$$

The first set of parameters gives a model for light-hole transitions, the second for heavy-hole transitions. τ was taken the same in both cases and corresponded roughly to the value we found for our measurements at 96 kOe. The results are given in Fig. 5. The oscillations in $G(\omega)$ have approximately $14\times$ larger amplitudes for light holes than for heavy holes. Since on the other hand the factor $(m_1+m_2)^2$ in Eq. (39) is about 16 times larger for heavy holes than for light holes, we expect the differential spectra to have comparable magnitudes for

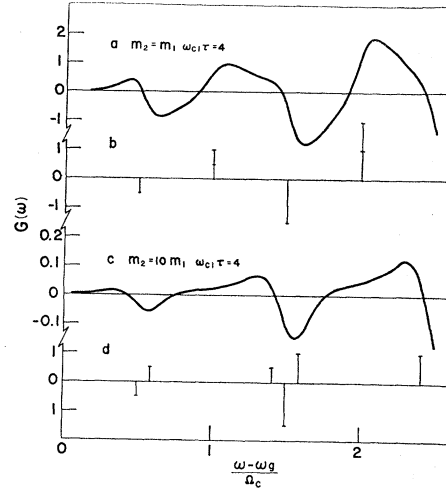


FIG. 5. The quantity $G(\omega)$ as defined in Eq. (39) for (a) $m_2=m_1$, $\omega_{c1}\tau=4$ and (c) $m_2=10m_1$, $\omega_{c1}\tau=4$. (b) and (d) show the calculated strengths and photon energies of individual lines in $G(\omega)$. The spectrum (a) is a model for light-hole-electron transitions and (c) for heavy-hole-electron transitions.

the two series of transitions. As already mentioned at the end of Sec. IV we have found the heavy-hole transitions to be somewhat stronger in the differential spectra than in the normal magnetoabsorption spectra when compared with the light-hole transitions. This probably indicates that the $\omega_{c1}\tau$ is actually somewhat larger than 4, the value used in these calculations.

VII. EXCITON STARK BROADENING

Up to this point we have discussed magnetoabsorption and cross-field magnetoabsorption neglecting exciton effects, i.e., neglecting the Coulomb interaction between electron and hole. However, excitons are known to affect the optical band edge strongly in the absence of a magnetic field,^{21,22} as well as the absorption lines in a magnetic field.^{23,24} The question thus arises how exciton effects might influence the differential magnetoabsorption spectra. In order to gain some insight into this problem we studied experimentally the effect of an electric field on the exciton absorption in zero magnetic field. We used a germanium sample backed to a glass substrate and therefore strained at 77°K, so that two exciton peaks were observed at this temperature.¹⁷ Two types of measurements were made. One consisted of measuring the absorption coefficient with an electric field applied to the sample. In the other we applied a dc electric field to the sample superimposed on which was a small ac field, so that differential spectra could be measured as a function of applied dc field. The re-

²¹ G. G. Macfarlane, T. P. McLean, J. E. Quarrington, and V. Roberts, Proc. Phys. Soc. (London) **71**, 863 (1958).

²² R. J. Elliott, Phys. Rev. **108**, 1384 (1957).

²³ R. J. Elliott and R. Loudon, J. Phys. Chem. Solids **15**, 196 (1960).

²⁴ D. F. Edwards and V. J. Lazazzera, Phys. Rev. **120**, 420 (1960).

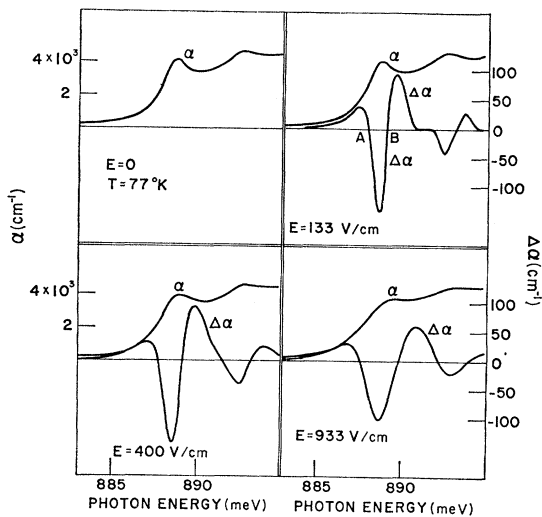


FIG. 6. Absorption and differential absorption in the direct exciton region in germanium at 77°K and for various values of applied dc electric field. Strain is present in the sample and consequently two exciton peaks are observed. The modulating voltage used for obtaining the differential spectra had a peak amplitude of 75 V/cm.

sults are shown in Fig. 6. The absorption data show that the exciton lines broaden in an electric field. At 933 V/cm the exciton absorption peaks have almost disappeared and merged into the continuum absorption. Stark broadening of exciton lines and their merging into the continuum was first observed by Gross²⁵ and others for higher members in the series in Cu₂O. The effect has been interpreted²⁶ as being due to field ionization of the exciton state. The theory of field ionization of excited states of the hydrogen atom has been treated by Lanczos.²⁷ His theory predicts the linewidth to be an exponential function of the applied electric field. The differential spectra are consistent with the picture of line broadening. We focus our attention on the dominant, i.e., lower energy exciton. The negative peak in the differential spectra coincides in energy with the exciton absorption peak at $E=0$, its position being very nearly independent of field up to 933 V/cm. If the effect of the electric field is to broaden the absorption line, without changing either its position or its line shape, then the difference in photon energy between the points A and B (see Fig. 6) of zero differential absorption at a given electric field E is proportional to the width of the absorption curve $\alpha(E)$. Actually, for a Gaussian line shape the difference in photon energy between A and B would be equal to the width of the absorption line between inflection points. We therefore define the width of the exciton line as the width of the differential curve between the points A and B . The width of the exciton

line defined in this way as a function of electric field is plotted in Fig. 7. It is seen that the width varies linearly with applied field. The slope of the straight line, which has the dimension of an electric dipole moment, is about 160(eV)cm/V, which is of the order of magnitude of the electron charge times the exciton radius. From the reduced effective mass for electron and heavy hole and the dielectric constant for germanium one calculates the Bohr radius of the exciton as ~ 210 Å. Lanczos's theory is valid only if $eER/\mathcal{E}_b \ll 1$, where E the electric field strength, R the radius, and \mathcal{E}_b the binding energy of the state from which field ionization takes place. [Note added in proof. Recently C. B. Duke and M. E. Alferieff have calculated the broadening of exciton lines by field ionization up to higher values of the electric field. {C. B. Duke, Phys. Rev. Letters 15, 625 (1965); C. B. Duke and M. E. Alferieff (to be published)}. The electric field strengths considered, however, are still mostly smaller than those in our experiment. The agreement

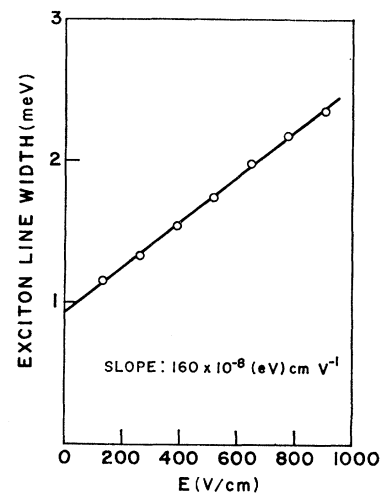


FIG. 7. The width of the lowest energy exciton line as a function of electric field. The slope of the straight line corresponds to an electric dipole moment of 1 electron charge at a distance of 160 Å.

between their theory and our experimental result is only qualitative, at best. The author is grateful to Dr. Duke for a stimulating discussion.] This requirement is not fulfilled in our measurements. We propose the following qualitative explanation of our results. Considering the exciton states as hydrogen atom like states Elliott¹⁸ has shown that optical excitation takes place only into S states. However, the width of the experimentally observed line, probably due to lifetime broadening, is about as large as the binding energy of the fundamental state, i.e., the lifetime τ is such that $\hbar/\tau \approx \mathcal{E}_{b0}$, \mathcal{E}_{b0} being the binding energy of the $1S$ state. In such a case the exciton states cannot properly be considered to be stationary hydrogen-like states. Rather, one would expect the states to be superpositions of stationary states for various quantum numbers n, l, m , the optical excitation still being to the S part of such a mixture. Insofar as mixtures of states of opposite parity are involved, these mixed states will have a finite elec-

²⁵ E. F. Gross, Progr. Phys. Sci. 63, 575 (1957).

²⁶ L. V. Keldysh, Zh. Eksperim. i Teor. Fiz. 34, 1138 (1958); [English transl.: Soviet Phys.—JETP 7, 788 (1958).]

²⁷ C. Lanczos, Z. Physik 62, 518 (1930); 65, 431 (1930); 68, 204 (1931).

tric dipole moment. The dipole moments will have a random orientation in space and their magnitudes will have a statistical distribution around some average, which we would expect to be of the order of electron charge times the Bohr radius for the exciton. An electric field will then broaden the line through a first-order effect of the electric field on the dipole moments. Thus, a broadening linear in E would result. Furthermore, one would expect the increase in linewidth to be of the order of $2\bar{p}E$ where \bar{p} is the average magnitude of the dipole moments.

As to the influence of exciton binding on the differential spectra we draw the following conclusions:

(1) If, as is most probably the case, absorption peaks in general correspond to exciton states connected with the Landau subbands, then the energies of the experimentally observed peaks, both for allowed and forbidden transitions, should be lower than those calculated for Landau transitions by the exciton binding energy, just as in the case of the normal magnetoabsorption.

(2) For forbidden transitions we had only one contribution to the differential spectrum, that due to the electric field induced transition probability. In the presence of exciton effects this will still be so, the Landau transition line shape now being replaced by an exciton line shape.

(3) For allowed transitions we had two contributions to the differential spectra, one resulting from a decrease in transition probability, the other from the electric field induced shift in transition energy. Both contributions are affected by exciton effects only in that the Landau line shape and its derivative should be replaced by the exciton line shape and its derivative. In addition, there may now be an effect due to line broadening, which will further change the line shape. However, the main feature of the differential spectrum for an allowed transition without exciton Stark broadening is a negative peak at the energy of the transition. The main feature of the differential spectrum for Stark broadening again is a negative peak at the energy of the exciton. The combined effect will thus again be mostly a negative peak at the energy of the transition (which, as mentioned under (1) is now modified by the exciton binding energy).

Thus we see that, even in the presence of exciton effects, the major features of a differential spectrum are positive peaks at the energies of forbidden transitions and negative peaks at the energies of allowed transitions. The conclusions we arrived at in the preceding section on the basis of Landau line shapes remain valid in the presence of exciton effects.

Finally, we mention that, for $H=0$, exciton structure can be observed more easily in a differential spectrum than in a normal absorption spectrum. In GaAs structure similar to that of Fig. 6 was found at room

temperature,²⁸ although no exciton lines could be observed in the normal absorption spectrum.

VIII. EXPERIMENTAL RESULTS FOR CROSS-FIELD MAGNETOABSORPTION

The bulk of the experimental results to be presented in this section are for a "strain-free" sample, for which we can readily compare theory with experiment. However, some data were taken on the strained sample that was also used for the exciton broadening experiments. Since the absorption lines were narrower in this sample, the differential spectra show more detail. On the other hand, we cannot very well compare these spectra with theory, the magnetic level structure in a strained sample not being known. Figure 8(a) shows the normalized transmission for σ_+ radiation, $\mathbf{H} \parallel [110]$, $H=44$ kOe both without an electric field and with a field of 900 V/cm applied to the sample. In the electric field a new dip in the transmission curve becomes apparent at about 908 meV; a direct observation of an electric field induced transition. Forbidden transitions are more clearly observed in the differential spectrum, as presented in Fig. 8(b). Here the allowed transitions show up as negative peaks, and a number of positive peaks indicate the presence of forbidden transitions. Unfor-

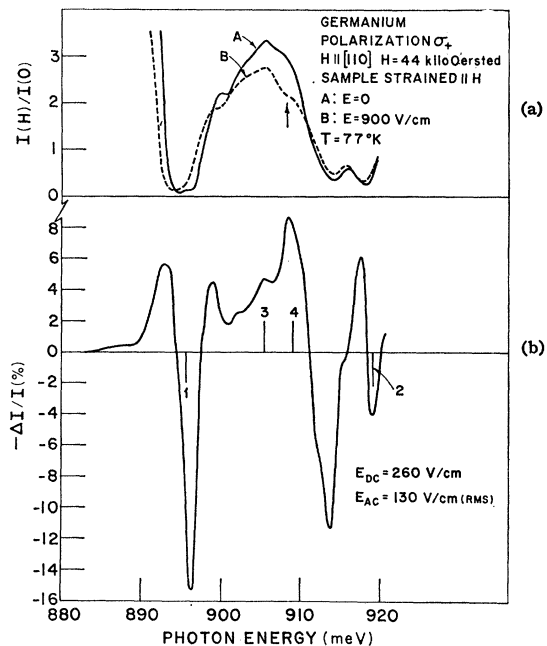


Fig. 8. Normalized transmission and differential absorption in a strained germanium sample at 77°K and $H=44$ 000 Oe. In the transmission curve B an extra, electric field induced absorption line is observed (see arrow). Forbidden transitions are more easily seen in the differential spectrum. The transitions (1) and (2) are allowed transitions, (3) and (4) are electric-field-induced forbidden transitions. Tentatively, the following assignment has been made: (1) $|b0+\rangle \rightarrow |0\beta\rangle$, (2) $|b1+\rangle \rightarrow |1\beta\rangle$, (3) $|b1+\rangle \rightarrow |0\beta\rangle$, and (4) $|b0+\rangle \rightarrow |1\beta\rangle$.

²⁸ Q. H. F. Vrehen, Bull. Am. Phys. Soc. 10, 534 (1965).

tunately, no complete theory is available for the magnetic level structure in a strained sample. Hasegawa²⁹ and co-workers have calculated the energies of the lowest transitions in germanium, with strain parallel to magnetic field and both parallel to $[110]$, including Coulomb binding effects. From their work it is apparent that the allowed transition, indicated as 1 in Fig. 8(b) is the transition $b0+ \rightarrow 0\beta$, i.e., from the zeroth light-hole level in the b series to the zeroth spin-down level in the conduction band. Comparison with the spectrum calculated for strain-free samples then suggests that 2 corresponds to $b1+ \rightarrow 1\beta$, and the forbidden transitions 3 and 4 to $b1+ \rightarrow 0\beta$ ($\Delta n = -1$) and $b0+ \rightarrow 1\beta$ ($\Delta n = +1$), respectively. In fact from the difference in energy for line 3 and 2 one calculates the electron mass in the conduction band as $m_1 = 0.037m$, in good agreement with the results of Roth *et al.*³ One also finds that the separation of the levels $n=0$ and $n=1$ in the light-hole b series equals $19.8 \times \hbar eH/mc$, in good agreement with the theoretical predictions for an unstrained sample. This experiment thus shows the possibility of deter-

mining electron and hole masses separately from differential spectra.

In Figs. 9(a) and 10(a) we present normalized transmission curves for germanium in a magnetic field of 96 kOe for σ_+ and σ_- radiation for a strain-free sample and $\mathbf{H} \parallel [110]$ at 77°K. Energies and strengths of the transitions were calculated with Roth's theory,³ including effects of higher than second order in k for the energies. The energy gap was treated as a parameter and determined by establishing the best fit for a number of the higher transitions, which are supposedly less influenced by exciton effects. Thus we found $\mathcal{E}_g = 883.3$ meV, which may be compared with 883.2 meV as determined by Macfarlane *et al.* This indicates the very good fit obtained. Also presented are the differential spectra, measured with $E_{dc} = 1000$ V/cm and $E_{ac} = 250$ V/cm (rms). Intensities of both allowed and forbidden transitions were calculated from the perturbation theory described in this paper. Allowed transitions are shown as negative, forbidden transitions as positive contributions to $\Delta\alpha$. These calculated spectra again do not include the effects due to electric-field-induced shifts in line position, i.e., the derivative contribution to $\Delta\alpha$ for allowed transitions has been neglected. In order to obtain a clear picture the calculated transition probabili-

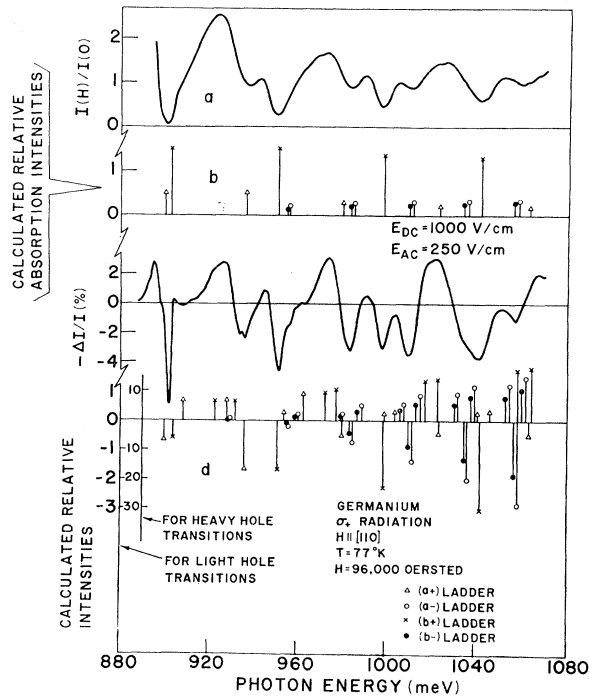


FIG. 9. Magnetoabsorption and cross-field differential absorption in "strain-free" germanium at 77°K and 96 kOe. $\mathbf{H} \parallel [110]$. Polarization σ_+ . (a) magnetoabsorption spectrum, (b) calculated absorption spectrum, (c) cross-field differential spectrum measured with $E_{dc} = 1000$ V/cm and $E_{ac} = 250$ V/cm (rms), and (d) calculated differential spectrum, the positive lines corresponding to forbidden transitions, the negative lines to allowed transitions. For clarity of presentation, the strengths of heavy-hole transitions are shown on a 10× smaller scale than those of light-hole transitions in the calculated spectrum (d). Note that heavy-hole transitions are relatively stronger in the differential spectrum than in the magnetoabsorption spectrum.

²⁹ H. Hasegawa (private communication).

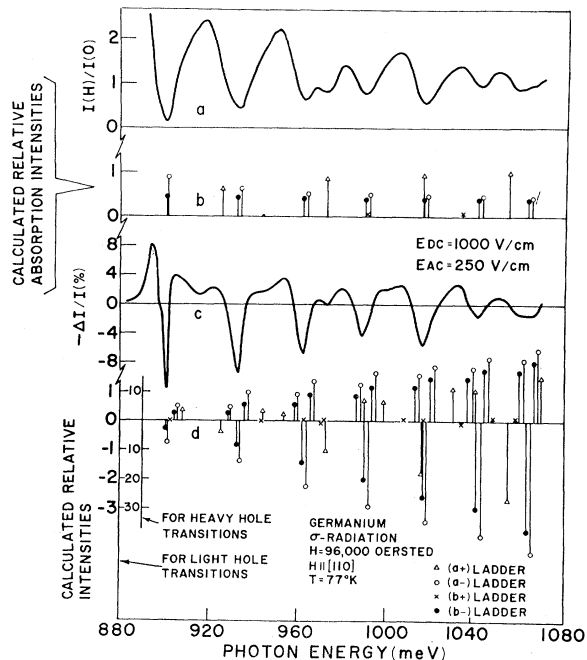


FIG. 10. Magnetoabsorption and cross-field differential absorption in "strain-free" germanium at 77°K and 96 kOe. $\mathbf{H} \parallel [110]$. Polarization σ_- . (a) magnetoabsorption spectrum, (b) calculated relative absorption intensities, (c) cross-field differential spectrum with $E_{dc} = 1000$ V/cm and $E_{ac} = 250$ V/cm (rms), and (d) calculated differential spectrum, positive lines corresponding to forbidden transitions, negative ones to allowed transitions. For clarity of presentation the strengths of heavy-hole transitions are shown on a 10× smaller scale than those of light-hole transitions in the calculated spectrum (d). Note that the differential spectrum is mainly due to the heavy-hole transitions and that this spectrum indeed resembles the calculated one of Fig. 5(c).

ties in the differential spectrum have been drawn on a ten times larger scale for light-hole transitions than for heavy-hole transitions. The following features can be seen from these figures:

(1) To each minimum in the transmission curve corresponds a negative peak in the differential spectrum. This shows that one can investigate the allowed transitions in a magnetoabsorption spectrum by studying the negative peaks in a differential spectrum. This is a very useful feature, since it has been found by the present author²⁸ that in GaAs magneto-optical oscillations could be detected with at least one order of magnitude better sensitivity by the differential method than by the normal magnetoabsorption method. As many as eight allowed transitions were observed at room temperature and 93 kOe.

(2) Both for σ_+ and σ_- radiation, it can be seen that allowed heavy-hole transitions are relatively stronger in the differential spectrum than in the normal absorption spectrum when compared with the allowed light-hole transitions. In the σ_+ spectrum one may compare the heavy-hole transitions at 983 and 1010 meV with the light-hole transition at 997 meV, in the σ_- spectra the heavy-hole transition at 963 meV with the light-hole one at 973 meV. The predominance of heavy-hole transitions, however, is not as large as predicted from the transition probabilities alone. These effects are in good agreement with the considerations put forward at the end of Sec. VI.

(3) The differential spectrum for σ_- radiation is dominated by heavy-hole transitions. This spectrum shows indeed a certain resemblance to the calculated one in Fig. 5.

(4) Although none of the forbidden transitions is resolved in the σ_+ spectrum, as they were in the case of the strained sample, the positive portions of the differential spectrum show a fairly good agreement with the calculated strengths of the forbidden transitions.

IX. CONCLUSIONS

Interband magnetoabsorption and magnetoreflexion measurements have yielded much information about the band structure of semiconductors and semimetals in recent years. From the theoretical and experimental results presented in this paper we may conclude that additional information can be derived from absorption

$$\begin{aligned} & -\Delta|\langle(na+)'|\sigma_-|(n-2, \alpha)'\rangle|^2 \\ & = |\langle(na+)'|\sigma_-|(n-3, \alpha)'\rangle|^2 + |\langle(na+)'|\sigma_-|(n-1, \alpha)'\rangle|^2 + E^2 C^2 \{ [(a_{1,n}^+)^2 - (a_{1,n-1}^+)^2] (V_{n,n-1}^{a++})^2 \\ & \quad + [(a_{1,n}^+)^2 - (a_{1,n+1}^+)^2] (V_{n,n+1}^{a++})^2 + [(a_{1,n}^+)^2 - (a_{1,n-1}^-)^2] (V_{n,n-1}^{a+-})^2 + [(a_{1,n}^+)^2 - (a_{1,n+1}^-)^2] (V_{n,n+1}^{a+-})^2 \\ & \quad - 2a_{1,n-1}^+ a_{1,n-1}^- V_{n,n-1}^{a++} + V_{n,n-1}^{a+-} - 2a_{1,n+1}^+ a_{1,n+1}^- V_{n,n+1}^{a++} + V_{n,n+1}^{a+-} \}. \quad (A1) \end{aligned}$$

For σ_+ radiation and transitions from light-hole levels in the a series,

$$\begin{aligned} & -\Delta|\langle(na+)'|\sigma_+|(n\alpha)'\rangle|^2 \\ & = |\langle(na+)'|\sigma_+|(n-1, \alpha)'\rangle|^2 + |\langle(na+)'|\sigma_+|(n+1, \alpha)'\rangle|^2 + \frac{1}{3} E^2 C^2 \{ [(a_{2,n}^+)^2 - (a_{2,n-1}^+)^2] (V_{n,n-1}^{a++})^2 \\ & \quad + [(a_{2,n}^+)^2 - (a_{2,n+1}^+)^2] (V_{n,n+1}^{a++})^2 + [(a_{2,n}^+)^2 - (a_{2,n-1}^-)^2] (V_{n,n-1}^{a+-})^2 + [(a_{2,n}^+)^2 - (a_{2,n+1}^-)^2] (V_{n,n+1}^{a+-})^2 \\ & \quad - 2a_{2,n-1}^+ a_{2,n-1}^- V_{n,n-1}^{a++} + V_{n,n-1}^{a+-} - 2a_{2,n+1}^+ a_{2,n+1}^- V_{n,n+1}^{a++} + V_{n,n+1}^{a+-} \}. \quad (A2) \end{aligned}$$

measurements in crossed electric and magnetic fields. First, from the photon energies of allowed ($\Delta n=0$) and forbidden ($\Delta n=\pm 1$) transitions, one can determine the effective mass of electron and hole separately. Secondly, the electric field affects heavy-hole-electron transitions more strongly than light-hole-electron transitions, which gives a means of distinguishing between these two types of transitions. This information was obtained with relatively low electric fields (<1000 V/cm). Not only is the use of low electric-field strengths experimentally convenient, it also allows the absorption coefficient to be calculated on the basis of a perturbation theory which can be applied equally well to a complicated band structure as to the case of simple parabolic bands. The results of this perturbation theory for germanium are in good agreement with the experimental differential spectra. Generally, differential spectra show more detail than the normal magnetoabsorption spectra. In GaAs it was found by the present author that magneto-oscillations in the interband optical absorption could be observed better in the cross-field differential spectra than in the magnetoabsorption spectra. This is probably true as well for other large energy-gap materials, that can be obtained in high-resistivity form. The results of the investigations reported in this paper then tell us how to interpret these differential spectra.

ACKNOWLEDGMENTS

The author would like to thank Professor Benjamin Lax for his interest in this investigation, Dr. H. Hasegawa for information on transition energies in strained germanium, R. N. Brown and C. R. Pidgeon for careful reading of the manuscript, and colleagues of the National Magnet Laboratory for many helpful discussions. The assistance of R. E. Newcomb in the experiments is much appreciated, as is the work of W. Tice of our Laboratory on the preparation of thin semiconductor samples.

APPENDIX A: TRANSFER OF TRANSITION PROBABILITY BY AN ELECTRIC FIELD

The decrease in transition probability for allowed transitions in an electric field to second power in E is approximately given by Eq. (25b) through Eq. (28b). We now present the full expressions: For σ_- , light holes in the a series,

For π transitions from a -series light-hole levels,

$$\begin{aligned} & -\Delta|\langle(na+)'|\pi|(n\beta)'\rangle|^2 \\ & = |\langle(na+)'|\pi|(n-1,\beta)'\rangle|^2 + |\langle(na+)'|\pi|(n+1,\beta)'\rangle|^2 + \frac{2}{3}E^2C^2\{[(a_{2,n^+})^2 - (a_{2,n-1^+})^2](V_{n,n-1}^{a^{++}})^2 \\ & \quad + [(a_{2,n^+})^2 - (a_{2,n+1^+})^2](V_{n,n+1}^{a^{++}})^2 + [(a_{2,n^+})^2 - (a_{2,n-1^-})^2](V_{n,n-1}^{a^{+-}})^2 + [(a_{2,n^+})^2 - (a_{2,n+1^-})^2](V_{n,n+1}^{a^{+-}})^2 \\ & \quad - 2a_{2,n-1^+}a_{2,n-1^-}V_{n,n-1}^{a^{++}}V_{n,n-1}^{a^{+-}} - 2a_{2,n+1^+}a_{2,n+1^-}V_{n,n+1}^{a^{++}}V_{n,n+1}^{a^{+-}}\}. \quad (\text{A3}) \end{aligned}$$

And finally, for π transitions from b -series light-hole levels,

$$\begin{aligned} & -\Delta|\langle(nb+)'|\pi|(n-2,\alpha)'\rangle|^2 \\ & = |\langle(nb+)'|\pi|(n-3,\alpha)'\rangle|^2 + |\langle(nb+)'|\pi|(n-1,\alpha)'\rangle|^2 + \frac{2}{3}E^2C^2\{[(b_{1,n^+})^2 - (b_{1,n-1^+})^2](V_{n,n-1}^{b^{++}})^2 \\ & \quad + [(b_{1,n^+})^2 - (b_{1,n+1^+})^2](V_{n,n+1}^{b^{++}})^2 + [(b_{1,n^+})^2 - (b_{1,n-1^-})^2](V_{n,n-1}^{b^{+-}})^2 + [(b_{1,n^+})^2 - (b_{1,n+1^-})^2](V_{n,n+1}^{b^{+-}})^2 \\ & \quad - 2b_{1,n-1^+}b_{1,n-1^-}V_{n,n-1}^{b^{++}}V_{n,n-1}^{b^{+-}} - 2b_{1,n+1^+}b_{1,n+1^-}V_{n,n+1}^{b^{++}}V_{n,n+1}^{b^{+-}}\}. \quad (\text{A4}) \end{aligned}$$

The various terms in the right-hand side of these equations all represent transfer of transition probability from the particular allowed transition to other transitions. We consider this in detail for $-\Delta|\langle(na+)'|\sigma_-|(n-2,\alpha)'\rangle|^2$ from Eq. (A1). The first two terms, which are the dominant ones, represent transfer of intensity to the forbidden transitions $n \rightarrow n-3$ and $n \rightarrow n-1$. The third and fourth terms are opposite to certain terms in

$$-\Delta|\langle(n-1,a+)'\sigma_-|(n-3,\alpha)'\rangle|^2 \quad \text{and} \quad -\Delta|\langle(n+1,a+)'\sigma_-|(n-1,\alpha)'\rangle|^2.$$

They therefore represent transfer of transition probability to other allowed σ_- transitions from light-hole levels in the a series. Similarly, the fifth and sixth terms represent transfer of intensity to allowed σ_- transitions from heavy-hole levels in the a series. To prove these statements one uses the fact that $(V_{n,n+1}^{a_{ij}})^2 = (V_{n+1,n}^{a_{ji}})^2$. Finally, the seventh and eighth terms in $-\Delta|\langle(na+)'|\sigma_-|(n-2,\alpha)'\rangle|^2$, $-\Delta|\langle(na+)'|\sigma_+|(n,\alpha)'\rangle|^2$, and $-\Delta|\langle(na+)'|\pi|(n,\beta)'\rangle|^2$ add up to zero since $a_{1,n^+}a_{1,n^-} + a_{2,n^+}a_{2,n^-} = 0$ because of the orthonormality of light- and heavy-hole states. These terms therefore represent transfer of intensity from the σ_- spectrum to the σ_+ and π spectra.

The third through eighth terms in Eqs. (A1)–(A4) are generally small. This is so because, on the one hand, factors like $(a_{1,n^+})^2 - (a_{1,n-1^+})^2$ are small since the a_{1,n^+} vary only gradually with n (and tend to a constant value for larger n), while, on the other hand, coefficients like $V_{n,n-1}^{a^{+-}}$ that express the coupling between light- and heavy-holes are also usually small, as was argued in Sec. IV.

Thus the right-hand side of Eqs. (A1)–(A4) can be approximated by the first two terms in these expressions, yielding Eqs. (25b) through (28b).

APPENDIX B

In evaluating an integral like (5) it is usually assumed^{2,3} that the envelope functions are varying slowly, so that the integral can be approximated by the product of an integral of the Bloch functions over the unit cell, and one of the envelope functions over the whole crystal, leading to (6). In the case of a magnetic field, however, k_x determines the center of the orbit y_0 by the relation $y_0 = k_x L_M^2$. Thus k_x is not necessarily small, and is not even confined to the first Brillouin zone. On the other hand, $\exp ik_x z$ and Φ_n have to be slowly varying functions for the effective mass approximation to be valid. For (5) to be different from zero one then obtains the requirement $k_{z_i}' = k_{z_i}$ and $k_{x_i}' = k_{x_i} + K_{x_i}$, where \mathbf{K}_i is a vector of the reciprocal lattice from which it follows:

$$\begin{aligned} & \int \Psi_{i_n'}^*(\mathbf{r}, k_{x_i} + K_{x_i}, k_{z_i}) eE y \Psi_{i_n}(\mathbf{r}, k_{x_i}, k_{z_i}) d\mathbf{r} \\ & = \frac{1}{V_0} \int_{\text{unit cell}} u_{i_0}^* u_{i_0} \exp(-iK_{x_i} x_i) d\mathbf{r} \int_{\text{crystal}} \Phi_n^* \left(\frac{y}{L_M} - (k_{x_i} + K_{x_i}) L_M \right) eE y \Phi_n \left(\frac{y}{L_M} - k_{x_i} L_M \right) d\mathbf{r}. \quad (\text{B1}) \end{aligned}$$

For $K_{x_i} = 0$ this is equivalent to (7). For $K_{x_i} \neq 0$, Φ_n' and Φ_n have the centers of their orbits at different values of y . The distance between the centers is $y_0' - y_0 = K_{x_i} L_M^2$, whereas the size of the orbit for Φ_n is of the order $L_M(2n+1)^{1/2}$. Therefore, when $K_{x_i} L_M \gg (2n+1)^{1/2}$ the overlap between the two functions will be very small and we may neglect matrix elements off-diagonal in k_x . The requirement $K_{x_i} L_M \gg (2n+1)^{1/2}$ for all $K_{x_i} \neq 0$ however, is implied in the assumption that the effective-mass approximation can be used.